

Fouling and Slagging Characteristics during Co-combustion of Coal and Biomass

Danchen Zhu, Haiping Yang, Yingquan Chen,* Zhi Li, Xianhua Wang, and Hanping Chen

The effects of different kinds (cotton stalk, rice husk, and sawdust) and proportions (0%, 10%, 20%, and 30% based on weight) of biomass and operating conditions (temperature and excess air coefficient) were evaluated relative to the ash deposition characteristics during the co-firing of Huang Ling (HL) coal with biomass. The experiments were performed in a drop-tube furnace. The chemical compositions and mineral phase characteristics of the collected ash particles were analyzed using scanning electron microscopy with energy dispersive X-ray (SEM-EDX) and X-ray diffraction (XRD), respectively. The results showed that the most severe agglomeration, from co-firing coal with cotton stalk, was due to the higher content of alkali metals, especially K. The amount of K in the ash increased with an increasing proportion of cotton stalk, and ultimately, agglomeration was more serious. When the combustion temperature increased from 1050 °C to 1300 °C, the dystectic solid compounds were transformed into eutectic compounds. The increased excess air coefficient accelerated the sulfur reaction, but did not relieve the heavy sintering. Consequently, limiting the content of biomass in the fuel blends, maintaining a lower combustion temperature, and a suitable level of excess air were determined to be necessary for the co-firing of coal and biomass.

Keywords: Slagging characteristics; Co-combustion; Huangling coal; Biomass

Contact information: State Key Laboratory of Coal Combustion, School of Power and Energy Engineering, Huazhong University of Science and Technology, 430074 Wuhan, China;

* *Corresponding author:* 307301564@qq.com

INTRODUCTION

Biomass is an ideal alternative to fossil fuels, as it can be grown in a sustainable way through a cyclical process of fixation and release of CO₂, which thereby helps to mitigate global warming problems (McKendry 2002). The co-firing of biomass and coal has been proposed as one of the most cost-effective technologies to use renewable materials on a large scale (Turn *et al.* 2006). There are many advantages to blending biomass with coal prior to burning. The emissions of SO_x and NO_x are reduced in most co-firing tests, depending on the biomass fuel used, and the CO₂ net production is also inherently lower because biomass is considered to be CO₂ neutral (Abreu *et al.* 2010).

Recently, investigation into the co-firing of fossil fuels with biomass has been drawing increasing attention because partial replacement of fossil fuels is possible in many cases. This fact alone gives extensive support to the growth of power sectors in developing countries (Sahu *et al.* 2014). Sometimes biofuel products are mixed with coal to achieve better control of the burning process (Wang *et al.* 2009). Burning biomass with

fossil fuels has a positive impact, both on the environment and on the economics of power generation.

However, biomass has high contents of easily vaporizable alkali metals and chlorine (Di Blasi 2008), which may result in several ash-related problems, such as fouling, slagging, corrosion, and bed agglomeration (Yang *et al.* 2014). Ash-related problems from co-combustion remain as longstanding challenges for co-firing coal and biomass, particularly agricultural residues, such as cereal straws, that contain high amounts of alkali/alkaline-earth metals (0.5 wt.% to 2 wt.% potassium) and chlorine (up to 0.2 wt.% to 1 wt.%) (Shao *et al.* 2012).

The behavior of alkali metals during combustion is known to have a direct correlation with ash-related problems and strongly depends on both the fuel composition and temperature (Knudsen *et al.* 2004; van Lith *et al.* 2008; Johansen *et al.* 2011). Many researchers have focused on the release of alkali metals during biomass combustion, but the co-firing process results in more complex agglomeration behavior due to the differences in the physical and chemical characteristics of the biomass and coal (Nystrom *et al.* 2017; Yang *et al.* 2014; Zhou *et al.* 2017). It might not be possible to predict the properties of the ash formed during co-combustion from the known characteristics of the ash formed from each fuel individually (Vamvuka and Kakaras 2011).

The blending ratio, fuel types, and operating conditions affect the ash components and ash features (Vamvuka *et al.* 2009). Wang *et al.* (2013) investigated the deposited behavior in a tube furnace and a Muffle furnace and discovered that the blending ratios of coal/straw caused different effects on the ash quantity. Shao *et al.* (2012) studied the co-combustion of lignite-peat blends in a bubbling fluidized bed combustor and found that the contents of the chlorine element, alkali/alkaline earth metals, SiO₂, and Al₂O₃ of the feed played a key role in the ash deposition. The deposited Ca, Mg, Al, and Si elements were present mostly in the forms of calcium and magnesium sulfates, aluminates, and silicates that have relatively low melting points (Qiu *et al.* 2014). Liao *et al.* (2015) found that under high temperature combustion conditions, alkali metal-related compounds, which had low melting points and easily condensed on the flue surface as fly ash, caused fouling and high temperature corrosion. Vassilev *et al.* (2010) studied the mineral differences between biomass and coal, and found some possible reversible coupling reactions between the minerals from the coal and chloride in the biomass during the co-firing process. However, the amounts of K and Na released during co-combustion could be reduced by the effects of Fe, Ti, S, Si, and Al from the blended fuels (Li *et al.* 2014).

There have been some studies focused on biomass alkalis or coal ash-related problems, which mainly investigated the biomass pyrolysis process (Keown *et al.* 2005), biomass combustion process (Liao *et al.* 2012), or coal combustion characteristics (Song *et al.* 2013; Wen *et al.* 2014, 2015, 2016). However, there has been no method accurate enough to evaluate the ash behavior during biomass co-firing until now, and the problem of slagging remains far from being solved. Moreover, the effect of blend ratios, combustion parameters, and biomass types during co-firing on the ash deposition behavior is still unclear.

The objective of this study was to investigate the effects of the blend ratio, temperature, and excess air coefficient on the fouling and slagging characteristics during co-combustion with cotton stalk. Then, the slagging characteristics of coal co-combusted with sawdust, rice husk, and cotton stalk at the same operating conditions were also studied. The chemical compositions, morphology, and mineral phase characteristics of the ashes were also analyzed using inductively coupled plasma (ICP), scanning electron

microscopy energy dispersive spectrometry (SEM-EDS), and X-ray diffraction (XRD), respectively. Semi-quantitative calculations were performed using the software HighScore to investigate the primary cause for ash deposition. The ash deposition behavior and transformation of the chemical compositions of the ashes from co-fired coal and biomass were considered.

EXPERIMENTAL

Materials

One typical Chinese coal Huang Ling bituminous coal sample (HL coal) (Huangling Mining (Group) Co., Ltd., Yanan, China) and three typical biomass samples (cotton stalk, rice husk, and sawdust) were used in this study. The biomass samples were pulverized and sieved into particles with sizes less than 100 μm , and the particles size range for coal was less than 80 μm . Prior to the experiments, the samples were oven-dried for 3 h at 55 $^{\circ}\text{C}$, and then the material was stored under dry conditions at room temperature.

The analyses of the experimental materials were conducted with a CHNS/O elemental analyzer (Vario MICRO cube, Elementar, Langensfeld, Germany). Proximate analysis was performed following the procedures specified in GB/T 28731 (2012), the standard of the proximate analysis of solid biofuels. The lower heating value (LHV) was determined using an oxygen bomb calorimeter (Parr6300, Parr Instrument Company, Moline, USA). The ash composition of all of the fuels were determined using an X-ray fluorescence spectrometer (EAGLEIII, EDAX Inc., Mahwah, USA).

The characterizations of the all of the fuels are listed in Table 1. Compared to the HL coal, the three kinds of biomass had high concentrations of chlorine and potassium in their ash, but lower sulfur contents. In addition, the sawdust had a much lower chlorine content compared to the cotton stalk and rice husk. With regards to the ash composition, the coal ash was rich in SiO_2 and Al_2O_3 (78.55%), the sawdust ash was made mostly up of SiO_2 and CaO (51.28%), the rice husk ash consisted mainly of SiO_2 (90.57%), and the cotton stalk ash mainly contained SiO_2 , CaO , and K_2O with some MgO and P_2O_5 .

Methods

The co-firing of the fuel blends was performed in a laboratory-scale drop-tube furnace (DTF). It included a fuel feeding system, high temperature furnace, and sampling probe, as shown in Fig. 1. The sample particles entrained in the gas were fed into the DTF by a Sankyo Piotech Micro Feeder (Model MFEV-10, Sankyo Piotech Co., Ltd., Sanda, Japan), and the feeding rate was 0.3 g/min for all of the runs. The height of the reactor tube was 2-m and the inner diameter was 56-mm. The DTF was electrically heated, and the wall temperature was monitored by thermocouples displayed on a monitor. The sampling probe was water-cooled with diluted nitrogen gas at the probe tip to prevent any secondary reactions of the char and ash. The details of our DTF system can be found elsewhere (Wen *et al.* 2013, 2014)

To ensure complete burning and reduce the impact of the unburned carbon, the primary air and secondary air were heated to 200 $^{\circ}\text{C}$ before entering the furnace. For each experiment, the stable combustion lasted 1 h or more with a continuous-feeding system, and the on-line flue gas analyzer was used to monitor the contents of O_2 and CO in the flue gas.

Table 1. Properties of the Fuels: Proximate Analysis, Ultimate Analysis, and Ash Analysis of the Materials

Parameter	Coal	Cotton Stalk	Rice Husk	Sawdust
Proximate Analysis (wt.%)				
Volatiles	32.32	74.95	60.35	78.21
Fixed Carbon	39.98	15.8	16.57	13.24
Moisture	2.79	4.66	6.33	4.56
Ash	24.91	4.59	16.75	3.99
LHV (MJ/kg)	22.29	17.77	13.76	17.2
Ultimate Analysis (wt.%)				
C	59.55	45.22	38.61	45.04
H	3.56	6.34	5.45	6.96
N	0.69	1.15	0.13	0.29
S	1.97	0.34	0.45	0.51
O*	6.53	37.7	32.28	38.65
Cl	0.00	0.13	0.11	0.02
Ash Analysis (wt.%)				
SiO ₂	47.32	18.79	90.57	20.42
CaO	6.77	26.93	0.84	30.86
Al ₂ O ₃	31.23	6.01	1.17	8.06
Fe ₂ O ₃	3.19	3.92	0.11	5.67
MgO	0.28	6.61	1.43	6.89
Na ₂ O	2.35	2.51	1.44	3.52
K ₂ O	0.71	17.62	1.95	9.62
P ₂ O ₅	0.88	7.37	1.06	3.00
TiO ₂	0.76	0.36	0.04	0.72
SO ₃	6.47	9.75	1.18	9.47
MnO ₂	0.04	0.13	0.21	1.77
*O was calculated as follows: O% = 100% – C% – H% – N% – S% – ash (%) – moisture (%)				

Altogether, the ashes were generated from 1 single fuel and 7 blended fuels in the experiments. The reaction temperature was set at 1050 °C and 1300 °C with excess air coefficients of 1.2 and 1.4. The fuels were burned in simulated air atmosphere (20 vol.% O₂/80 vol.% N₂). The contents of the coal and biomass in the fuel blends and control conditions used in the experiments are shown in Table 2. After combustion, most fly ash particles were blown and condensed on the water-cooled sampling probe. The rest of the fly ash particles were blown into the glass fiber filter with pore size of 0.3 μm at the outlet of sampling probe. Both the ash particles were collected, blended well in the filter for further analysis.

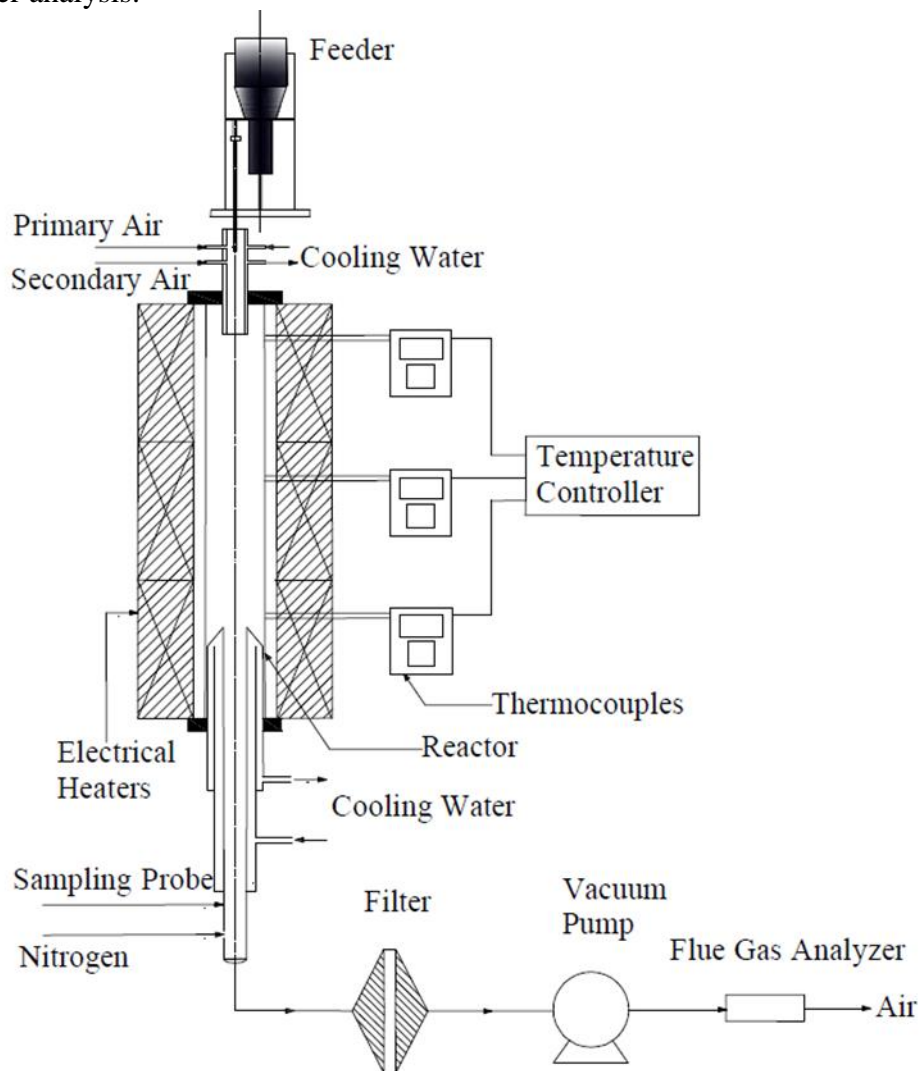


Fig. 1. Schematic diagram of the experimental setup

Table 2. Biomass Ratios, Temperatures, and Excess Air Coefficients of the Fuel Blends

Fuel No.	Sample	Biomass Ratio (%)	Temperature (°C)	Excess Air Coefficient (EAC)
#1	Coal	0	1300	1.2
#2	Coal + Cotton stalk	10	1300	1.2
#3	Coal + Cotton stalk	20	1300	1.2
#4	Coal + Cotton stalk	30	1300	1.2
#5	Coal + Cotton stalk	20	1050	1.2
#6	Coal + Cotton stalk	20	1300	1.4
#7	Coal + Rice husk	20	1300	1.2
#8	Coal + Sawdust	20	1300	1.2

Characterization of Ash and Slagging

The collected samples of slag from the combustion experiments were further characterized with SEM (Quanta 200, FEI, Eindhoven, Netherlands) combined with EDS and XRD (X'Pert Pro, PANalytical B.V., Almelo, Netherlands). The XRD spectra were obtained to analyze the slagging characteristics that resulted from the combustion process. The software X'Pert Highscore Plus (Version 2.0, PANalytical B.V., Almelo, Netherlands) was used in the semi-quantitative calculation of the content of the crystalline compound in the slag and ash. According to the PDF (2004) cards published by The International Centre for Diffraction Data (ICDD), the sample was mixed with α -Al₂O₃ at a ratio of 1:1 by weight, and thus, the ratio of the intensity of the strongest peak of the sample and corundum was called the RIR value, as shown in Eq. 1. By the principle of the adiabatic method, if there are N phases in a system, then the relative content of crystalline compounds can be calculated by Eq. 2. In this investigation, because the content of the Si element was conserved, the relative content of crystalline compounds in the ash could be calculated by using Eq. 3,

$$RIR_i = I_i / I_{col} \quad (1)$$

$$W_i = \frac{I_i / RIR_i}{\sum_{i=1}^N I_i / RIR_i} \quad (2)$$

$$W_i = \left(\frac{I_i}{RIR_i} \times \beta \right) / \sum_{i=1}^N \left(\alpha_i \times \frac{I_i}{RIR_i} \right) \quad (3)$$

where RIR_i is the ratio of the intensity of the strongest peak of the sample and corundum, I_i and I_{col} are the integrated intensities of the strongest peak of the sample and corundum, respectively, W_i is the relative content of the crystalline compounds (%), N is the number of phases in a system, α_i is the mass fraction of the Si element in the molecular weight of each phase (%), and β is the content of Si in the slag and ash (%).

RESULTS AND DISCUSSION

Effect of Biomass Blending Ratio

Figure 2 shows the SEM photomicrographs of the ash specimens from the co-firing of coal with cotton stalk ratios of 0%, 10%, 20%, and 30%. As for the coal ash from the DTF, shown in Fig. 2(a), the fine sticky particles acted like a glue to stimulate the sintering behavior of the ash. Additionally, spongy and irregular particles were also present. Comparing Fig. 2(b) to Fig. 2(a), it was seen that the co-firing of coal and biomass enhanced the sintering degree of the ash. Parts of the ash particles melted into large spherical particles, and other fine particles adhered to those particles. When the blending ratio rose to 20%, it was seen that severe agglomeration was caused because the ash was fully molten in the DTF, which was suggested by the spherical shape of the ash particles. When the ratio reached 30%, the combustion retention fused and condensed, and a compact nonporous globule was formed. The results indicated that the fusible composition in the ash increased, and the ash agglomeration tendency was promoted by the biomass being in excess of 20% cotton stalk. Therefore, it was reasonable to speculate that, when co-firing with HL coal, the blending ratios should be limited to 20% or less of cotton stalk.

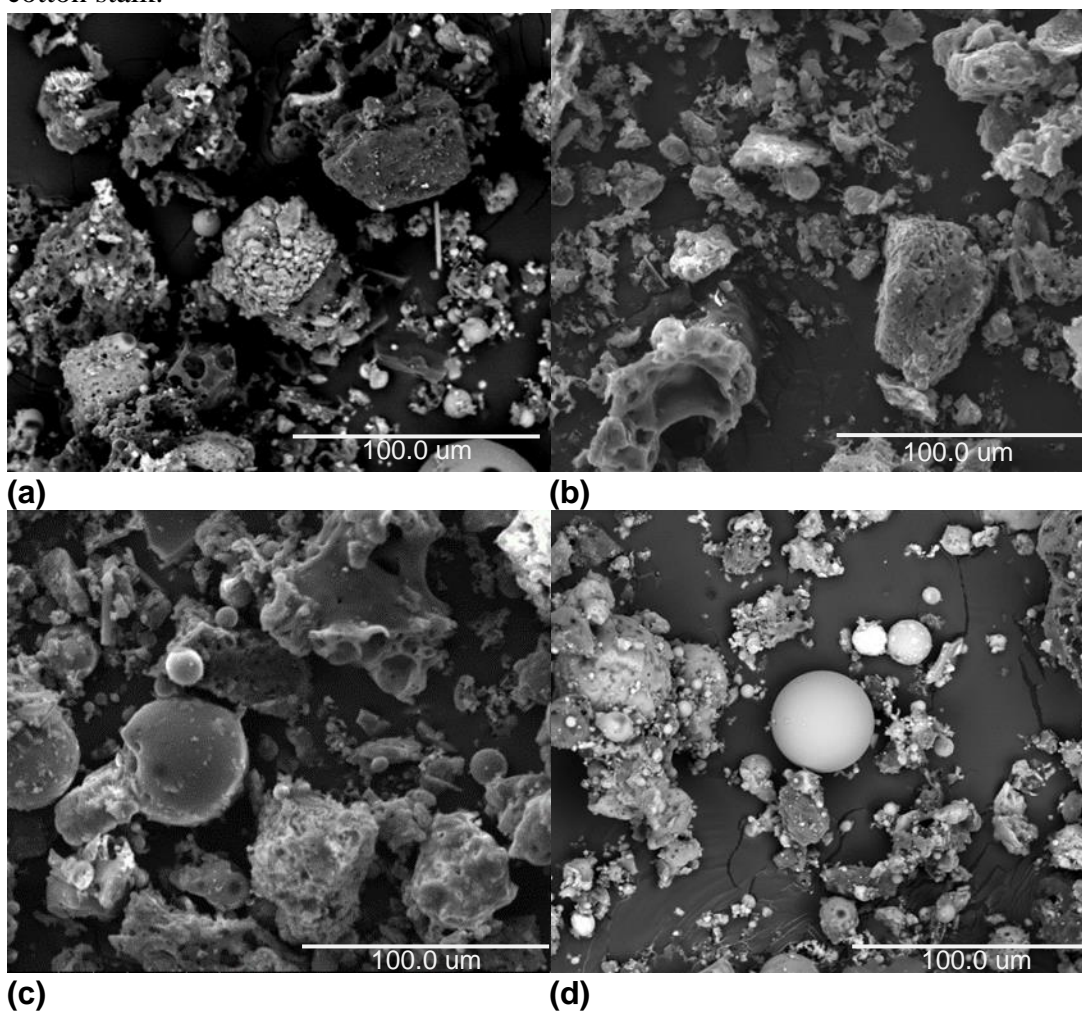


Fig. 2. SEM images of the ashes from coal co-fired with varying amounts of cotton stalk; (a) coal, (b) coal and 10% cotton stalk, (c) coal and 20% cotton stalk, and (d) coal and 30% cotton stalk

Table 3. Elemental Composition Results from EDS of the Ash Deposits

Element	Coal	Coal + 10% Cotton Stalk	Coal + 20% Cotton Stalk	Coal + 30% Cotton Stalk
Na (%)	0.16	0.24	0.49	0.62
Mg (%)	0.26	0.22	0.30	0.32
Al (%)	13.99	11.20	10.25	8.23
Si (%)	50.85	32.15	25.29	22.13
K (%)	0.48	3.12	4.80	6.20
Ca (%)	10.17	15.23	18.48	21.20
Fe (%)	3.09	18.32	24.97	28.13
Cl (%)	0.10	0.14	0.24	0.48
S (%)	0.82	0.81	1.21	1.85

The results of the EDS analysis are shown in Table 3. When the ratio of blending increased from 0% to 30%, the concentrations of K, Ca, Na, Fe, and Cl clearly increased, and the concentrations of Si and Al decreased. This was in accordance with the large amount of alkali metals in the ash of the cotton stalk, and with the more severe agglomeration that was seen. And it was observed that the alkali metal enrichment of the slag caused the agglomeration to become more serious as the blending ratio increased. This was similar to the results of Müller *et al.* (2006). A difference from the coal combustion was noted that there was a clear iron content increase when biomass was co-combusted with coal. According to the increasing chlorine contents, It was speculated that some of chlorides in fly ashes might deposit on the cold surface of the probe as used in this study, thereby causing high temperature corrosion in the combustor (Hansen *et al.* 1999, Li *et al.* 2014, Shao *et al.* 2012). Thus, the iron on the sampling probe was transformed into Fe_2O_3 and collected into ash samples, which led to the significant Fe contents increasing in EDS results. According to the results of the XRD analysis, shown in Fig. 3 and Table 4, KAlSi_2O_6 (6.78% to 7.2%) and $\text{CaAl}_2\text{Si}_2\text{O}_8$ (20.37% to 28.43%) were detected in the blending slag with a ratio of 10%. When the blending ratio was increased from 10% to 30%, the content of detected KAlSi_2O_6 and $\text{CaAl}_2\text{Si}_2\text{O}_8$ both increased. It was also observed that when the cotton stalk content was higher than 30%, some KCl was detected. Wei *et al.* (2005) found that chlorine could increase the volatility of the alkali metal elements.

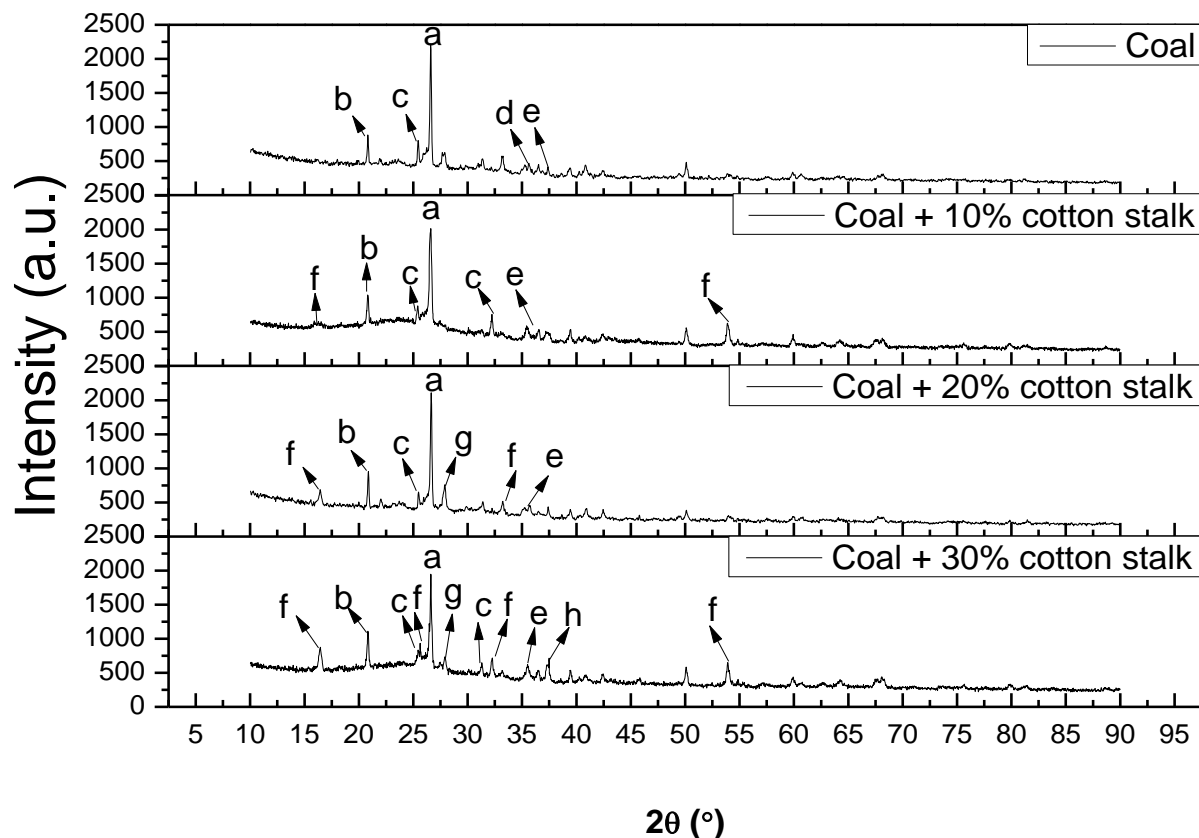


Fig. 3. XRD spectra of the ash co-fired with varying blending ratios, where *a* is quartz (SiO_2), *b* is aluminum phosphate (AlPO_4), *c* is anhydrite (CaSO_4), *d* is calcium oxide (CaO), *e* is hematite (Fe_2O_3), *f* is leucite (KAlSi_2O_6), *g* is anorthite ($\text{CaAl}_2\text{Si}_2\text{O}_8$), and *h* is sylvite (KCl)

Yang *et al.* (2014) showed that the content of the alkali vapor was mainly affected by the chlorine content rather than by the alkali metal itself. Another study dealt with the release and transformation of alkali metal species co-combustion of coal and S-rich wheat straw. It was found that the releasing processes of Cl and alkali metals were consistent at high temperatures, and it was apparent that there were chlorides formed with the emission of alkali metals (Li *et al.* 2014). Therefore, with the high content of K in the mixed fuel, some KCl was produced in the early combustion stage. Nevertheless, due to the short residence time, the KCl did not react with the Si and Al completely but was vaporized and condensed onto the ash particles. The melting point of KCl (776 °C) is much lower than that of KAlSi_2O_6 , and so, KCl reacted easily with SiO_2 to form a low melting point compound, which lowered the melting point of the slag residual. Thus, in the burning process, the higher blending ratios caused the release of KCl that attached to the surface of the ash particles, which led to serious agglomeration. Hence, as the blending ratio increased, the content of alkalis in the biomass increased, the content of formed KAlSi_2O_6 increased, the melting point of the ashes was lowered, and ultimately, more serious agglomeration occurred.

Table 4. Chemical Compositions from XRD Analysis for the Deposited Ashes

Si (wt.%)	Intensity	RIR	Integrated Intensity	Mass fraction
(Coal + 10% Cotton Stalk 1300 °C) 20.66%	SiO ₂	2.8 to 3.32	642	27.78% to 32.61%
	KAlSi ₂ O ₆	3.02 to 3.24	152	6.78% to 7.2%
	CaAl ₂ Si ₂ O ₈	0.41 to 0.72	93	20.37% to 28.43%
(Coal + 20% Cotton Stalk 1300 °C) 19.31%	SiO ₂	2.8 to 3.32	419	20.57% to 24.15%
	KAlSi ₂ O ₆	3.02 to 3.24	228	11.54% to 12.25%
	CaAl ₂ Si ₂ O ₈	0.41 to 0.72	100	24.85% to 34.68%
(Coal + 30% Cotton Stalk 1300 °C) 17.96%	SiO ₂	2.8 to 3.32	340	15.47% to 18.16%
	KAlSi ₂ O ₆	3.02 to 3.24	315	14.77% to 15.68%
	CaAl ₂ Si ₂ O ₈	0.41 to 0.72	115	26.48% to 36.95%
	KCl	8.28	-	-

Effect of Combustion Temperature

Figure 4 shows the microstructure of the ash and slag for coal that was co-combusted with 20% cotton stalk at 1050 °C and 1300 °C.

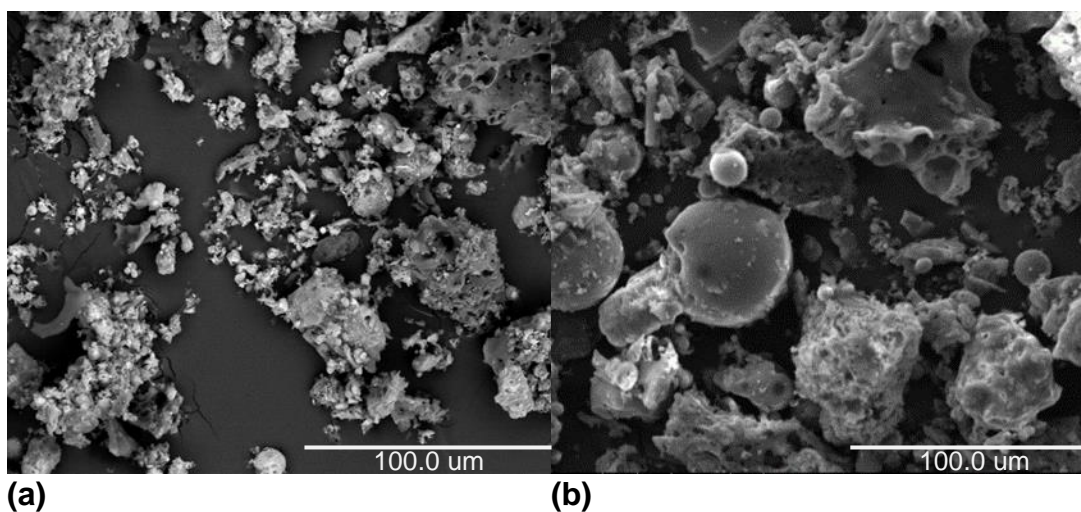


Fig. 4. SEM images of the ashes co-combusted (Coal + 20% cotton stalk, EAC = 1.2) at (a) 1050 °C and (b) 1300 °C

As shown in Fig. 4, when the combustion temperature was 1050 °C, there were many small particles present, and most of the ash particles were loose, spongy, and irregular. No obvious sintering was found. When the temperature increased from 1050 °C to 1300 °C, the spherical shape of the ash particles suggested that the ash was fully molten. It was seen that an increased co-combustion temperature enhanced the sintering degree of the ash.

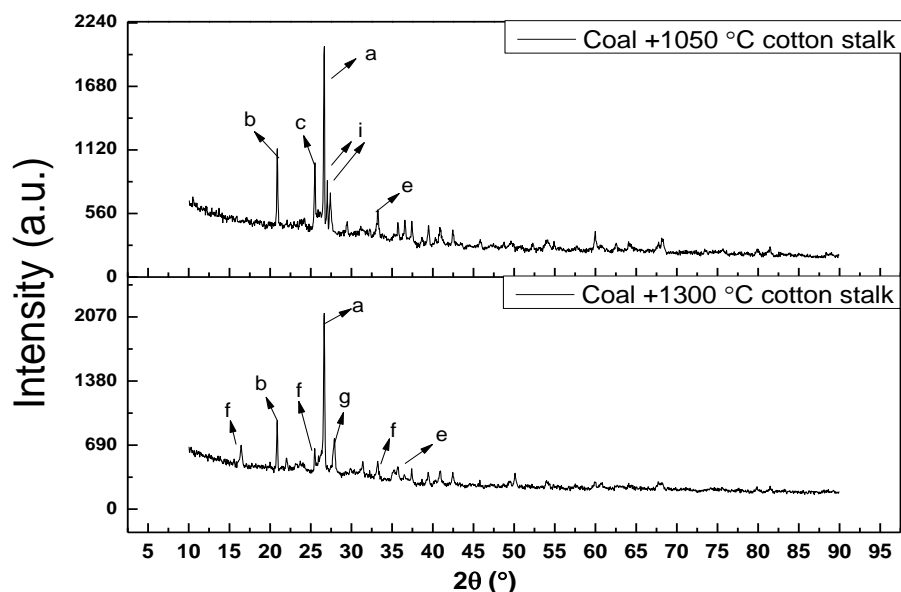
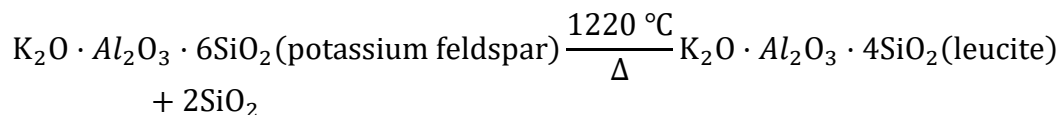


Fig. 5. XRD analysis of the ash deposits from different combustion temperatures, where *a* is quartz (SiO_2), *b* is aluminum phosphate (AlPO_4), *c* is anhydrite (CaSO_4), *e* is hematite (Fe_2O_3), *f* is leucite (KAlSi_2O_6), *g* is anorthite ($\text{CaAl}_2\text{Si}_2\text{O}_8$), and *i* is potassium feldspar (KAlSi_3O_8)

As shown in Fig. 5, the slag samples were analyzed with XRD. The potassium and calcium mainly existed in the form of KAlSi_3O_8 (melting point of $1290\text{ }^\circ\text{C}$) and CaSO_4 in the slag, respectively, when the temperature was $1050\text{ }^\circ\text{C}$, but they were in the form of KAlSi_2O_6 and $\text{CaAl}_2\text{Si}_2\text{O}_8$ in the slag, respectively, when the temperature was $1300\text{ }^\circ\text{C}$. Because the melting point of KAlSi_3O_8 is $1100\text{ }^\circ\text{C}$, the KAlSi_3O_8 did not reach the melting point when the temperature was $1050\text{ }^\circ\text{C}$, but it melted when the temperature was $1300\text{ }^\circ\text{C}$. Additionally, it reacted with the SiO_2 and generated a eutectic crystalline compound (KAlSi_2O_6), which has a melting temperature that is lower than that of KAlSi_3O_8 and CaSO_4 . The KAlSi_2O_6 was the main compound that lowered the ash melting temperature. Subsequently, when the combustion temperature increased from $1050\text{ }^\circ\text{C}$ to $1300\text{ }^\circ\text{C}$, the following reaction was speculated to have taken place:



This reaction was used to predict that potassium feldspar transforms into leucite at the noted temperature of $1220\text{ }^\circ\text{C}$. When the temperature increased from $1050\text{ }^\circ\text{C}$ to $1300\text{ }^\circ\text{C}$, this transformation occurred. In addition, at the higher temperature, more fusible components were generated, which caused more agglomeration.

Effect of Excess Air Coefficient

There were not many differences in the surface morphology and microstructure of the co-fired slag when the excess air coefficient increased from 1.2 to 1.4, and so, the SEM image was not displayed in this paper. Table 5 shows the elemental composition of the slag when co-combusted with different excess air coefficients. The results showed that the content of S increased with a higher excess air coefficient. This was possibly because more S was fixed in the reaction when it reacted with the alkali and alkaline

metals. However, the sulfur-fixed reaction did not change the melting characteristics of the ash and slag, and there were no noticeable changes to their physical appearance.

Table 5. Elemental Composition Results from EDS of the Ash Deposits at 1050 °C and with Different Excess Air Coefficients

	Coal + 20% Cotton Stalk (1.2 EAC)	Coal + 20% Cotton Stalk (1.4 EAC)
Na (%)	0.49	0.41
Mg (%)	0.30	0.32
Al (%)	10.25	11.20
Si (%)	25.29	32.15
K (%)	4.80	4.12
Ca (%)	18.48	16.23
Fe (%)	24.97	18.32
Cl (%)	0.24	0.14
S (%)	1.21	2.14

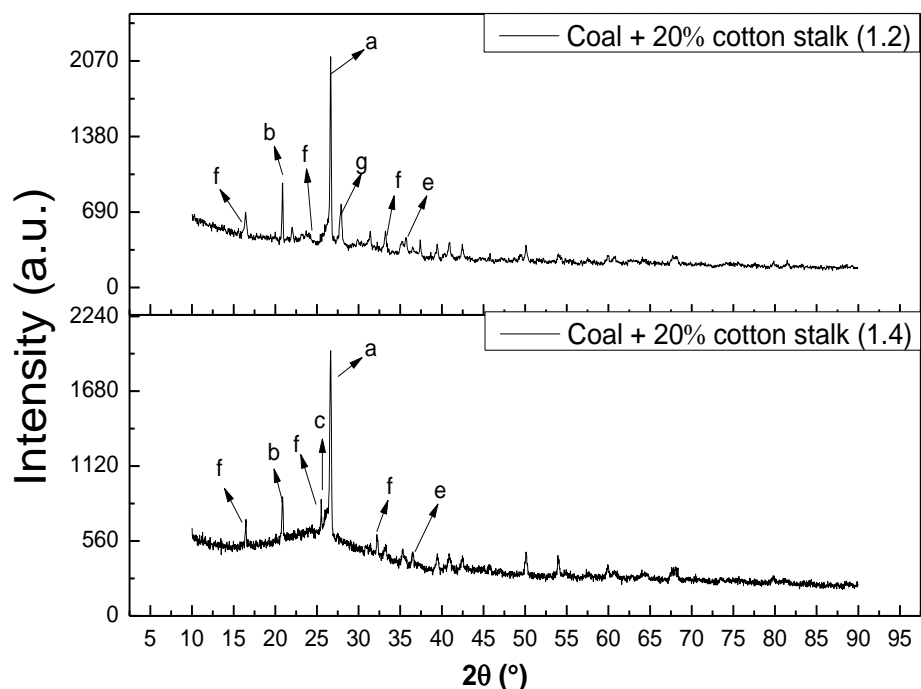


Fig. 6. XRD analysis of the ash samples (temperature = 1300 °C), where *a* is quartz (SiO_2), *b* is aluminum phosphate (AlPO_4), *c* is anhydrite (CaSO_4), *e* is hematite (Fe_2O_3), *f* is leucite (KAISi_2O_6), and *g* is anorthite ($\text{CaAl}_2\text{Si}_2\text{O}_8$)

In Fig. 6, when the excess air coefficient increased to 1.4, the diffraction peak of K_2SO_4 in the XRD spectrum of the slag did not appear, and the $\text{CaAl}_2\text{Si}_2\text{O}_8$ transformed into CaSO_4 , which was the main existing form of Ca. The reason for that may have been that K_2SO_4 was not stable at high temperatures, and it broke down to release SO_2 (Johansen *et al.* 2011). When the excess air coefficient was increased, an excess of O_2 could promote the sulfation reaction, especially during the step for the formation of SO_3

(Theis *et al.* 2006). Thus, S may be captured by Ca compounds, the formation of stable sulfates CaSO_4 is the dominant reaction path (Aho and Ferrer 2005; Li and Fang 2015; Mueller *et al.* 2006; Xiao *et al.* 2017). At the high temperature condition, the oxidation environment and the presence of Fe, Si, and Al remarkably promoted the sulfur fixation reaction of Ca. The CaSO_4 was considered to bond effectively between the particles, thus increasing the slagging tendency. Thus, the higher excess air coefficient accelerated the sulfur reaction, but did not relieve the heavy sintering.

Effect of Biomass Type

Figure 7 shows the SEM photographs of the microstructures of the four ash samples. For pure coal, the photographs showed some small particles on the surface, and no serious melting and agglomeration. However, combustion of the fuels with biomass added in (biomass/coal = 20 wt.%) enhanced the sintering degree of the ash.

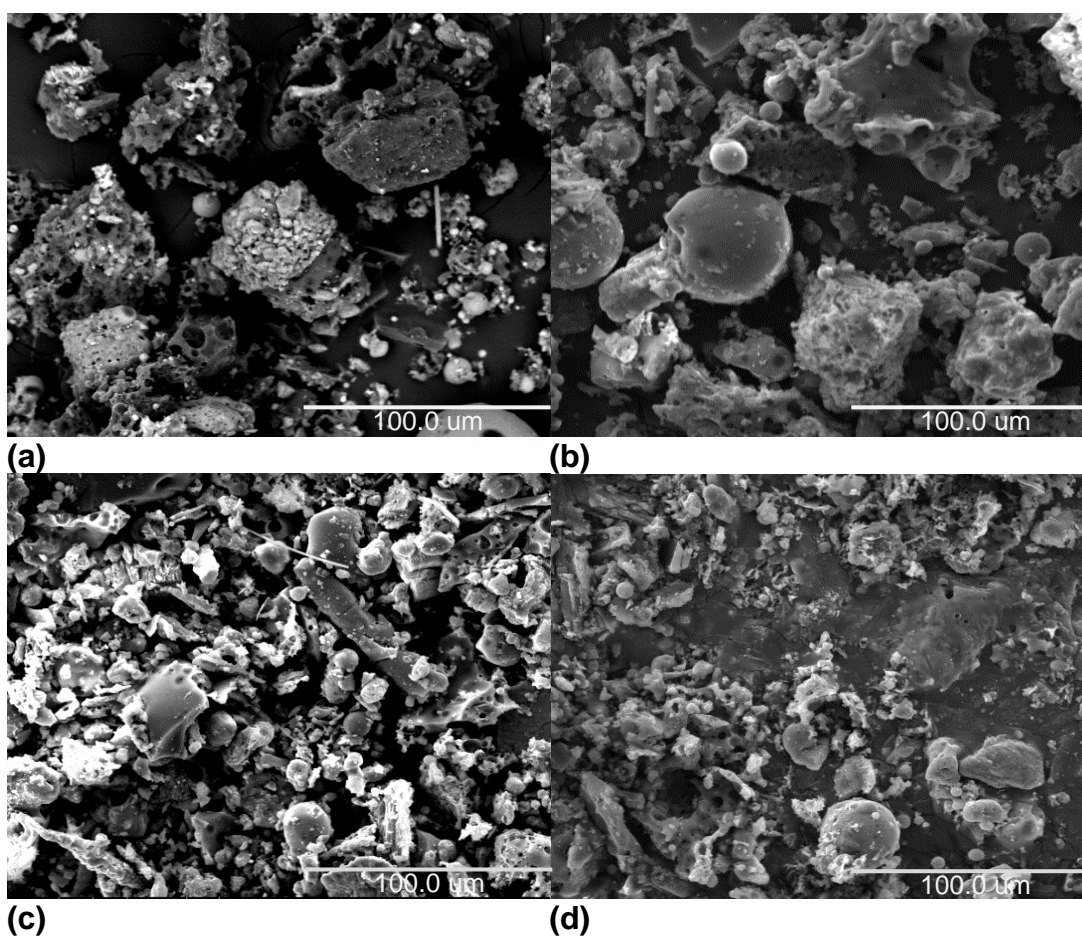


Fig. 7. SEM images of the ashes of (a) coal, (b) coal and 20% cotton stalk, (c) coal and 20% rice husk, and (d) coal and 20% sawdust

It is worth noting that the slag deposited from coal combusted with 20% cotton stalk had a compact morphology with larger blocks and less debris, and the surface of the blocks was smooth and dense. It was speculated that there were some compounds with low melting points generated in this ash sample. The phenomenon indicated that low melting point compounds played an important role in the slagging and fouling process. However, there was a big difference between the ash samples co-fired of coal/rice husk

blends and coal/cotton stalk blends. Its particles were smaller, broken, and formed a loose structure. The morphology of the slag from coal co-fired with sawdust had more agglomeration than that of the slag from coal co-fired with rice husk and less than that of the slag from coal co-fired with cotton stalk.

Table 6 shows the EDS results of different ash samples. The Al, Si, Ca, and Fe were the main inorganic elements, and there were limited amounts of Na, Mg, K, Cl, and S. The samples of adhered fouling from the coal combustion and coal co-combusted with 20% rice husk both had very high amounts of Si, but there was more Na, Mg, and K in the coal co-fired with rice husk. The slag of the co-combusted cotton stalk had the highest contents of K, Fe, Cl, and S, and the lowest contents of Si and Al. Mi *et al.* (2004) found that the biomass had a higher alkaline oxide content with higher ion potential energy than the coal, and the polymer compounds were damaged during the melting of the ash. Hence, the addition of biomass decreased the melting point of the ash. Therefore, the severe agglomeration caused by the cotton stalk addition might have been due to the higher content of alkali metal elements, especially K. Meanwhile in the coal ash and coal-rice husk ash, the content of silicon was 53%, and the alkali metals content was lower. This was in accordance with the SEM photographs in Figs. 2(a) and 2(c). The element contents of the co-combusted sawdust were between the element contents found for cotton stalk and rice husk, except for the contents of Na and Ca, which were the highest, and the S content, which was the lowest.

Table 6. Elemental Composition Results from EDS of the Ash Deposits

	Coal	Coal + 20% Cotton Stalk	Coal + 20% Rice Husk	Coal + 20% Sawdust
Na (%)	0.16	0.49	0.43	0.52
Mg (%)	0.26	0.30	0.41	0.31
Al (%)	13.99	10.25	12.28	10.96
Si (%)	50.85	25.29	53.00	27.74
K (%)	0.48	4.80	1.12	2.11
Ca (%)	10.17	18.48	6.75	21.39
Fe (%)	3.09	24.97	5.20	16.78
Cl (%)	0.10	0.24	0.22	0.23
S (%)	0.82	1.21	1.08	1.03

The XRD results of the ash particles are shown in Fig. 8 and Table 7. The major crystalline compound present in the slag during coal combustion was SiO₂. However, after introducing the cotton stalk, there was not only SiO₂ observed in the deposits, but also, CaAl₂Si₂O₈ and KAlSi₂O₆. The content of KAlSi₂O₆ was much higher, and the content of SiO₂ was lower than in the other co-combusted ashes. This was in accordance with the lower Si content and higher K content of the coal-cotton stalk ash in Table 6.

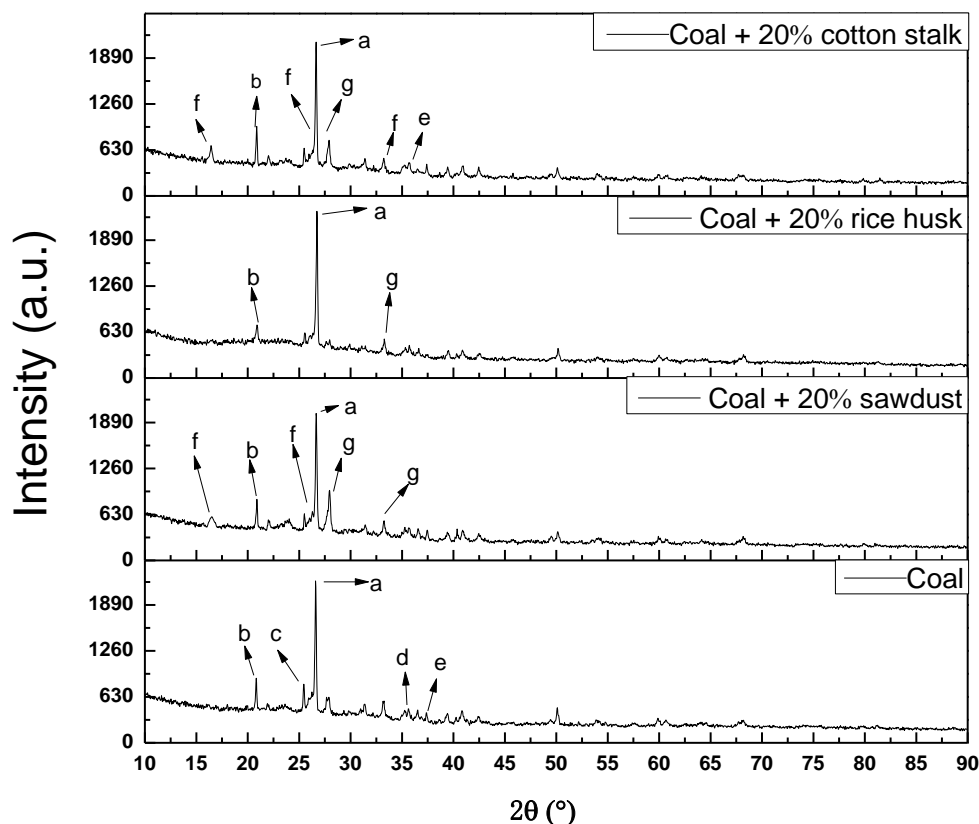


Fig. 8. XRD analysis of the ash deposits co-fired with different biomasses, where *a* is quartz (SiO_2), *b* is aluminum phosphate (AlPO_4), *c* is anhydrite (CaSO_4), *d* is calcium oxide (CaO), *e* is hematite (Fe_2O_3), *f* is leucite (KAlSi_2O_6), and *g* is anorthite ($\text{CaAl}_2\text{Si}_2\text{O}_8$)

Table 7. Chemical Compositions of the Deposited Ashes

Si (wt.%)	Intensity	RIR	Integrated Intensity	Mass Fraction
(coal + 20% Cotton Stalk 1300 °C) 19.31%	SiO_2	2.8 to 3.32	419	20.57% to 24.15%
	KAlSi_2O_6	3.02 to 3.24	228	11.54% to 12.25%
	$\text{CaAl}_2\text{Si}_2\text{O}_8$	0.41 to 0.62	100	24.85% to 34.68%
(coal + 20% Rice Husk 1300 °C) 26.04%	SiO_2	2.8 to 3.32	714	45.20% to 52.82%
	KAlSi_2O_6	3.02 to 3.24	0	0.00
	$\text{CaAl}_2\text{Si}_2\text{O}_8$	0.41 to 0.62	43	13.72% to 19.15%
(coal + 20% Sawdust 1300 °C) 19.15%	SiO_2	2.8 to 3.32	620	23.12% to 27.14%
	KAlSi_2O_6	3.02 to 3.24	160	6.15% to 6.53%
	$\text{CaAl}_2\text{Si}_2\text{O}_8$	0.41 to 0.62	131	24.73% to 34.51%

Wei *et al.* (2002) showed that KAlSi_2O_6 (leucite) has a low melting point (about 1100 °C), and it easily melts with SiO_2 to form glassy, sticky, and fusible compounds, which noticeably enhances the cohesiveness between the ash particles. Additionally, Fe_2O_3 was detected in the coal-cotton stalk ash. Russell *et al.* (2002) reported that Fe_2O_3 very effectively fluxes with aluminosilicates, which lowers the melting point and viscosity of the ash. Thus, the presence of Fe_2O_3 promoted the ash deposition behavior. The major compounds in the ash of coal co-combusted with sawdust were KAlSi_2O_6 and $\text{CaAl}_2\text{Si}_2\text{O}_8$. Because the $\text{CaAl}_2\text{Si}_2\text{O}_8$ (anorthite) has the highest melting point and a favorable thermal stability in feldspar minerals, it did not help to generate fusible compounds. The major compounds present in the ash formed by coal co-combusted with rice husk were SiO_2 and $\text{CaAl}_2\text{Si}_2\text{O}_8$. And the main mineral in coal ash are quartz (SiO_2), anhydrite (CaSO_4), and CaO . All of these compounds had higher melting points, and there were no fusible compounds detected, such as KAlSi_2O_6 . By comparison, the CaSO_4 and CaO have relatively higher viscosity than $\text{CaAl}_2\text{Si}_2\text{O}_8$, and they play a role of glue to stimulate the agglomeration behavior of the ash (Luan *et al.* 2014). Therefore the agglomeration of ash from coal and rice husk blend fuel (shown in Figure 7 (c)) is less than that from pure coal.

According to the above analysis, when coal was co-fired with cotton stalk, the content of KAlSi_2O_6 increased, which implied that the ash deposition tendency was considerably promoted by the biomass, which had a higher content of potassium. Therefore, it was reasonable to presume that, from the degree of agglomeration, when co-firing with biomass, the K content in the blending fuel should be limited.

CONCLUSIONS

1. Co-firing coal and biomass is an effective technology for reducing the net emission of CO_2 . The properties of co-fired coal and biomass vary widely, causing complexity in the ash deposition behavior. The results of this study showed how different blending ratios, combustion temperatures, excess air coefficients, and different biomass types affected the slagging characteristics and composition of the ash.
2. The content of the alkali metal K in the biomass was found to be one of the critical factors in determining the characteristics of the blended fuel ashes. When co-firing coal with different proportions of cotton stalk, the degree of deposited ash increased with the increasing cotton stalk ratio in the fuel blends. To avoid ash deposition problems, the content of cotton stalk in the fuel blends should be limited to 20%.
3. The sintering characteristics of ash were related to the chemical compositions. When the combustion temperature was low, the K was mainly found in KAlSi_3O_8 in the ashes. Then, the KAlSi_3O_8 was converted to KAlSi_2O_6 after the temperature increased to above 1220 °C. This increased the adhesion of the slag particles and decreased the melting point. Hence, when co-firing with 20% cotton stalk, to prevent ash-related problems, the combustion temperature should be no higher than 1220 °C. When the excess air coefficient was increased at the high temperature, S preferred to react with Ca and created CaSO_4 , rather than fixing the K element into K_2SO_4 . This reaction only changed the ash composition, and

had no effects on the melting characteristics.

4. After comparing the characteristics of the ash from co-firing with cotton stalk, rice husk, and sawdust, the most severe agglomeration was seen in the ashes from co-firing with cotton stalk, and no obvious sintering was found in the ash from the coal co-fired with rice husk. Co-firing with sawdust caused a middle degree of agglomeration in the ash.

ACKNOWLEDGMENTS

The authors wish to express great appreciation for the financial support from the National Natural Science Foundation of China (51476067 and 51376067), the National Basic Research Program of China (2013CB228102), the Special Fund for Agro-scientific Research in the Public Interest (201303095), and the Fundamental Research Funds for the Central Universities, HUST (CX15-019). This study also benefited from the assistance of the experimental studies support from the Analytical and Testing Center at Huangzhong University of Science and Technology.

REFERENCES CITED

- Abreu, P., Casaca, C., and Costa, M. (2010). "Ash deposition during the co-firing of bituminous coal with pine sawdust and olive stones in a laboratory furnace," *Fuel* 89(12), 4040-4048. DOI: 10.1016/j.fuel.2010.04.012
- Aho, M., and Ferrer, E. (2005). "Importance of coal ash composition in protecting the boiler against chlorine deposition during combustion of chlorine-rich biomass," *Fuel* 84(2-3), 201-212. DOI: 10.1016/j.fuel.2004.08.022
- Di Blasi, C. (2008). "Modeling chemical and physical processes of wood and biomass pyrolysis," *Prog. Energ. Combust.* 34(1), 47-90. DOI: 10.1016/j.pecs.2006.12.001
- GB/T 28731 (2012). "Proximate analysis of solid biofuels," Standardization Administration of China, Beijing, China.
- Hansen, L. A., Frandsen, F. J., Dam-Johansen, K., Sorensen, H. S. and Skrifvars, B. J. (1999). "Characterization of ashes and deposits from high-temperature coal-straw co-firing." *Energy & Fuels*, 13(4), 803-816. DOI: 10.1021/ef980203x.
- ICDD (2004). "Powder diffraction file," International Center for Diffraction Data, Pennsylvania, USA
- Johansen, J. M., Jakobsen, J. G., Frandsen, F. J., and Glarborg, P. (2011). "Release of K, Cl, and S during pyrolysis and combustion of high-chlorine biomass," *Energ. Fuel.* 25(11), 4961-4971. DOI: 10.1021/ef201098n
- Keown, D. M., Favas, G., Hayashi, J. I., and Li, C. Z. (2005). "Volatilisation of alkali and alkaline earth metallic species during the pyrolysis of biomass: Differences between sugar cane bagasse and cane trash," *Bioresour Technol.* 96(14), 1570-1577. DOI: 10.1016/j.biortech.2004.12.014
- Knudsen, J. N., Jensen, P. A., and Dam-Johansen, K. (2004). "Transformation and release to the gas phase of Cl, K, and S during combustion of annual biomass," *Energ. Fuel.* 18(5), 1385-1399. DOI: 10.1021/ef049944q

- Li, F., and Fang, Y. (2015). "Modification of ash fusion behavior of lignite by the addition of different biomasses," *Energy & Fuels* 29(5), 2979-2986. DOI: 10.1021/acs.energyfuels.5b00054.
- Li, R., Kai, X., Yang, T., Sun, Y., He, Y., and Shen, S. (2014). "Release and transformation of alkali metals during co-combustion of coal and sulfur-rich wheat straw," *Energ. Convers. Manage.* 83, 197-202. DOI: 10.1016/j.enconman.2014.02.059
- Liao, Y., Cao, Y., Chen, T., and Ma, X. (2015). "Experiment and simulation study on alkalis transfer characteristic during direct combustion utilization of bagasse," *Bioresource Technol.* 194, 196-204. DOI: 10.1016/j.biortech.2015.06.121
- Liao, Y., Yang, G., and Ma, X. (2012). "Experimental study on the combustion characteristics and alkali transformation behavior of straw," *Energ. Fuel.* 26(2), 910-916. DOI: 10.1021/ef2016107
- Luan, C., You, C. F., and Zhang, D. K. (2014). "Composition and sintering characteristics of ashes from co-firing of coal and biomass in a laboratory-scale drop tube furnace," *Energy* 69, 562-570. DOI: 10.1016/j.energy.2014.03.050
- McKendry, P. (2002). "Energy production from biomass (part 1): Overview of biomass," *Bioresource Technol.* 83(1), 37-46. DOI: 10.1016/S0960-8524(01)00118-3
- Mi, T., Chen, H., Wu, Z., Liu, D., Zhang, S., Wu, C., and Chang, J. (2004). "Chemistry characteristic study on biomass ash," *Acta Energiæ Solaris Sinica* 25(2), 236-241.
- Müller, M., Wolf, K. -J., Smeda, A., and Hilpert, K. (2006). "Release of K, Cl, and S species during co-combustion of coal and straw," *Energ. Fuel.* 20(4), 1444-1449. DOI: 10.1021/ef0600356
- Nystrom, R., Lindgren, R., Avagyan, R., Westerholm, R., Lundstedt, S., and Boman, C. (2017). "Influence of wood species and burning conditions on particle emission characteristics in a residential wood stove," *Energy & Fuels* 31(5), 5514-5524. DOI: 10.1021/acs.energyfuels.6b02751.
- ICDD (2004). "Powder diffraction file," International Center for Diffraction Data, Pennsylvania, USA
- Qiu, K., Zhang, H., Zhou, H., Zhou, B., Li, L., and Cen, K. (2014). "Experimental investigation of ash deposits characteristics of co-combustion of coal and rice hull using a digital image technique," *Appl. Therm. Eng.* 70(1), 77-89. DOI: 10.1016/j.applthermaleng.2014.04.063
- Russell, N. V., Wigley, F., and Williamson, J. (2002). "The roles of lime and iron oxide on the formation of ash and deposits in PF combustion," *Fuel* 81(5), 673-681. DOI: 10.1016/S0016-2361(01)00154-5
- Sahu, S. G., Chakraborty, N., and Sarkar, P. (2014). "Coal-biomass co-combustion: An overview," *Renew. Sust. Energ. Rev.* 39, 575-586. DOI: 10.1016/j.rser.2014.07.106
- Shao, Y., Xu, C., Zhu, J., Preto, F., Wang, J., Tourigny, G., Badour, C., and Li, H. (2012). "Ash and chlorine deposition during co-combustion of lignite and a chlorine-rich Canadian peat in a fluidized bed - Effects of blending ratio, moisture content and sulfur addition," *Fuel* 95, 25-34. DOI: 10.1016/j.fuel.2011.12.020
- Song, W., Tang, L., Zhu, Z., and Ninomiya, Y. (2013). "Rheological evolution and crystallization response of molten coal ash slag at high temperatures," *AIChE J.* 59(8), 2726-2742. DOI: 10.1002/aic.14052

- Theis, M., Skrifvars, B.-J., Zevenhoven, M., Hupa, M. and Tran, H. (2006). "Fouling tendency of ash resulting from burning mixtures of biofuels. Part 2: Deposit chemistry," *Fuel*, 85(14-15), 1992-2001. DOI: 10.1016/j.fuel.2006.03.015.
- Vamvuka, D., and Kakaras, E. (2011). "Ash properties and environmental impact of various biomass and coal fuels and their blends," *Fuel Process. Technol.* 92(3), 570-581. DOI: 10.1016/j.fuproc.2010.11.013
- Vamvuka, D., Pitharoulis, M., Alevizos, G., Repouskou, E., and Pentari, D. (2009). "Ash effects during combustion of lignite/biomass blends in fluidized bed," *Renew. Energ.* 34(12), 2662-2671. DOI: 10.1016/j.renene.2009.05.005
- Van Lith, S. C., Jensen, P. A., Frandsen, F. J., and Glarborg, P. (2008). "Release to the gas phase of inorganic elements during wood combustion. Part 2: Influence of fuel composition," *Energ. Fuel*. 22(3), 1598-1609. DOI: 10.1021/ef060613i
- Vassilev, S. V., Baxter, D., Andersen, L. K., and Vassileva, C. G. (2010). "An overview of the chemical composition of biomass," *Fuel* 89(5), 913-933. DOI: 10.1016/j.fuel.2009.10.022
- Wang, C., Wang, F., Yang, Q., and Liang, R. (2009). "Thermogravimetric studies of the behavior of wheat straw with added coal during combustion," *Biomass. Bioenerg.* 33(1), 50-56. DOI: 10.1016/j.biombioe.2008.04.013
- Wang, C., Xu, C., Cao, Z., and Di, H. (2013). "Investigation on minerals migration during co-firing of different straw/coal blending ratios," *Energ. Convers. Manage.* 74, 279-285. DOI: 10.1016/j.enconman.2013.04.040
- Wei, X., Lopez, C., Von Puttkamer, T., Schnell, U., Unterberger, S., and Hein, K. R. G. (2002). "Assessment of chlorine-alkali-mineral interactions during co-combustion of coal and straw," *Energ. Fuel*. 16(5), 1095-1108. DOI: 10.1021/ef0102925
- Wei, X. L., Schnell, U., and Hein, K. R. G. (2005). "Behaviour of gaseous chlorine and alkali metals during biomass thermal utilisation," *Fuel* 84(7-8), 841-848. DOI: 10.1016/j.fuel.2004.11.022
- Wen, C., Gao, X. P. and Xu, M. H. (2016). "A CCSEM study on the transformation of included and excluded minerals during coal devolatilization and char combustion," *Fuel*, 172, 96-104. DOI: 10.1016/j.fuel.2016.01.005.
- Wen, C., Xu, M. H., Zhou, K., Yu, D. X., Zhan, Z. H., and Mo, X. (2015). "The melting potential of various ash components generated from coal combustion: Indicated by the circularity of individual particles using CCSEM technology," *Fuel Processing Technology* 133, 128-136. DOI: 10.1016/j.fuproc.2015.01.012.
- Wen, C., Yu, D., Wang, J., Wu, J., Yao, H., and Xu, M. (2014). "Effect of the devolatilization process on PM10 Formation during oxy-fuel combustion of a typical bituminous coal," *Energy & Fuels* 28(9), 5682-5689. DOI: 10.1021/ef501264v.
- Wen, C., Xu, M., Yu, D., Sheng, C., Wu, H., Zhang, P. a., Qiao, Y. and Yao, H. (2013). "PM10 formation during the combustion of N2-char and CO2-char of Chinese coals." *Proceedings of the Combustion Institute* 34(2), 2383-2392. DOI: 10.1016/j.proci.2012.07.080.
- Xiao, H., Li, F., Liu, Q., Ji, S., Fan, H., Xu, M., Guo, Q., Ma, M., and Ma, X. (2017). "Modification of ash fusion behavior of coal with high ash fusion temperature by red mud addition," *Fuel* 192, 121-127. DOI: 10.1016/j.fuel.2016.12.012.

Yang, T., Kai, X., Li, R., Sun, Y., and He, Y. (2014). “The behavior of alkali metals during the co-combustion of straw and coal,” *Energy Sources Part A-Recovery Utilization and Environmental Effects* 36(1), 15-22. DOI: 10.1080/15567036.2011.629278

Zhou, C., Liu, G., Xu, Z., Sun, H., and Lam, P. K. S.(2017). “The retention mechanism, transformation behavior and environmental implication of trace element during co-combustion coal gangue with soybean stalk,” *Fuel* 189, 32-38. DOI: 10.1016/j.fuel.2016.10.093.

Article submitted: February 16, 2017; Peer review completed: June 10, 2017; Revised version received: July 11, 2017; Accepted: July 12, 2017; Published: July 17, 2017.
DOI: 10.15376/biores.12.3.6322-6341